



Archived by Flinders University

This is the peer reviewed version of the following article:

Pedler, R., Harris, J., Thomson, N., Buss, J., Stone, D., & Handlinger, J. (2022). Development of a semi-quantitative scoring protocol for gill lesion assessment in greenlip abalone *Haliotis laevigata* held at elevated water temperature. In *Diseases of Aquatic Organisms* (Vol. 150, pp. 37–51). Inter-Research Science Center.

Which has been published in final form at:

<https://doi.org/10.3354/dao03673>

Copyright © 2022 Inter-Research.

1

2 Gill lesion assessment in greenlip abalone (*Haliotis laevis*) held at elevated water temperature.

3

4 Histopathology of *Haliotis laevis* gills

5

6 R. L. Pedler¹, J. O. Harris^{1,5*}, N. L. Thomson², J. J. Buss^{1,3}, D. A. J. Stone^{1,2,4,5}, J. H. Handler⁶

7 ¹ College of Science and Engineering, Flinders University, Bedford Park, 5042, South Australia,

8 Australia.

9 ² School of Animal and Veterinary Sciences, The University of Adelaide, Roseworthy, 5371, South

10 Australia, Australia.

11 ³ Department of Primary Industries and Regions, Fisheries and Aquaculture, West Beach, 5024,

12 South Australia, Australia.

13 ⁴ South Australian Research and Development Institute, West Beach, 5024, South Australia,

14 Australia.

15 ⁵ Marine Innovation Southern Australia, West Beach, SA, 5024, South Australia, Australia.

16 ⁶ Institute of Marine and Antarctic Studies, University of Tasmania, Hobart, 7001, Tasmania

17 Australia.

18 **Abstract**

19 Water temperatures which exceed thermal optimal ranges (~19-22°C for greenlip abalone (*Haliotis*
20 *laevigata*), depending on stock genetics) can be associated with abalone mortalities. We assessed
21 histopathological changes in *H. laevigata* gills held in control (22°C) or elevated (25°C) water
22 temperature conditions for 47 days by developing a new scoring protocol which incorporates
23 histopathological descriptions and relative score summary. Lesions were allocated to one of three
24 reaction patterns: (1) epithelial, (2) circulatory or (3) inflammatory and scored based on their
25 prevalence in gill leaflets. Indices for each reaction pattern were calculated and combined to
26 provide an overall gill index. *Haliotis laevigata* held in 25°C water temperature had significantly
27 more epithelial lifting and hemolymph channel enlargement and significantly higher gill and
28 circulatory reaction pattern indices than *H. laevigata* held in 22°C water temperature. Only live or
29 moribund *H. laevigata* were assessed; therefore, lesions are not necessarily reflective of abalone
30 mortality. One *H. laevigata* had proliferation of un-identified cells in the v-shaped skeletal rod of a
31 gill leaflet. The un-identified cells contained enlarged nuclei, a greater nucleus-cytoplasm ratio and
32 in some cases, mitotic figures. This cell population could represent a region of haematopoiesis in
33 response to hemocyte loss or migration to a lesion. Without thorough diagnostic testing, the origin
34 of these larger cells cannot be confirmed. The new scoring protocol developed will allow the
35 standard quantification of gill lesions for *H. laevigata*, specifically for heat-related conditions, and
36 could further be adapted for other *Haliotis* spp..

37 **Keywords:** hemocytes, abalone, gill histopathology, summer mortality, scoring protocol.

38 1. INTRODUCTION

39

40 Greenlip abalone (*Haliotis laevis*) are economically important shellfish cultured in South
41 Australia. In 2017/2018, the South Australian abalone aquaculture industry produced 399 tonnes of
42 abalone valued at \$14.2 million AUD and contributed ~\$42.3 million AUD to the state economy
43 (BDO EconSearch 2019). *Haliotis laevis* are commonly cultured in land-based systems which
44 are subject to large fluctuations in water temperature (10°C to 25°C) (Stone et al. 2013, Stone et al.
45 2016). When water temperatures increase beyond those optimum for *H. laevis* growth (~19-
46 22°C, depending on stock genetics), farms can experience abalone mortality events for weeks
47 afterwards referred to by farmers and in literature as summer mortality. Research in stock genetics
48 has allowed for better understanding of *H. laevis* susceptibility to summer mortality; Shiel et al.
49 (2020) identified 487 *H. laevis* genes which express differently for abalone tolerant to thermal
50 stress than abalone susceptible to thermal stress. During a 75 day laboratory induced heat wave
51 experiment involving water temperatures of 18°C, 20°C and 21°C, 54 genes were significantly
52 differentially expressed (Shiel et al. 2020). Data from Shiel et al. (2020) supports potential of
53 selective breeding and genetic improvement programs to decrease the stock mortalities (of up to
54 50%) (Vandepier 2006, Stone et al. 2013) and economic losses which can be associated with
55 summer mortality. Research and implementation of genetic improvement programs for *H. laevis*
56 remains in its infancy and studies that offer practical solutions to summer mortality now are crucial
57 (Shiel et al. 2018).

58

59 Water temperature-related mortality events in molluscs are common and represent an interaction
60 between infectious and non-infectious disease (Cheng et al. 2004a, Travers et al. 2008a).
61 Temperature-related mortality events have been described for various cultured *Haliotis* spp.,
62 including summer immune depression in the European green ormer (*Haliotis tuberculata*) (Travers
63 et al. 2008a) and bacterial disease outbreaks in the culture of small Taiwan abalone (*Haliotis*

64 *diversicolor supertexta*) (Cheng et al. 2004a) and *H. laevigata*, *H. ruba* and their hybrids in
65 Tasmania (Handlinger et al., 2005). Withering syndrome is a disease affecting *Haliotis* spp. caused
66 by *Xenohaliotis californiensis* whereby bacterial cells infect and damage abalone epithelial cells in
67 the gastrointestinal tract which can lead to starvation and death in abalone (Braid et al. 2005,
68 Friedman et al. 1997). While a direct relationship between withering syndrome in *Haliotis* spp. and
69 water temperature has not been identified, elevated water temperatures likely play a role in
70 exacerbating mortalities (Braid et al. 2005, Friedman et al. 1997).

71

72 *Haliotis* spp. are ectothermic, meaning their metabolism is directly affected by environmental water
73 temperature (Abele & Puntarulo 2004, Lushchak 2011, Vosloo et al. 2013). Increased water
74 temperature can increase the metabolic activity, oxygen and energy demand of *Haliotis* spp.
75 (Vandeppeer 2006, Day et al. 2010, Lushchak 2011). Elevated metabolic activity increases the
76 production of reactive oxygen species (ROS) as a by-product of cellular respiration (Vosloo &
77 Vosloo 2010, Lushchak 2011, Hooper et al. 2014b). Harmful ROS are primarily stabilised by
78 endogenous antioxidant enzymes, which are produced in response to oxidative stress (De Zoysa et
79 al. 2008, 2009, Lushchak 2011, Lange et al. 2014). When endogenous antioxidants in *Haliotis* spp.
80 are depleted, the antioxidant/ROS balance becomes de-stabilised, resulting in excess ROS
81 (Lushchak 2011). Excess ROS can damage abalone deoxyribonucleic acid (DNA), proteins and
82 lipids, specifically the oxidation of polyunsaturated fatty acids (Abele & Puntarulo 2004, Lushchak
83 2011). The cellular damage induced by ROS can manifest as changes to *Haliotis* spp. cell structure,
84 necrosis and tissue damage (Lushchak 2011) which have been observed in previous
85 histopathological studies of thermal stress in *Haliotis* spp. (Day et al. 2010, Hooper et al. 2014b).

86

87 Infection with *Vibrio* spp. bacteria (vibriosis) is often associated with *Haliotis* spp. summer
88 mortality (Nicolas et al. 2002, Pichon et al. 2013, Cardinaud et al. 2015, Handlinger et al. 2015).
89 *Vibrio* spp. optimally grow in 30°C water temperature (Travers et al. 2008a). High bacterial

90 abundance of *Vibrio* spp. and depression of *Haliotis* spp. immune systems in warmer water
91 temperature (Nicolas et al. 2002, Cheng et al. 2004a, Travers et al. 2009, Hooper et al. 2014b) is the
92 likely cause of more *Vibrio* spp. infections in abalone during summer. *Haliotis* spp. possess an
93 innate immune system containing both cellular and humoral components (De Vico & Carella 2012).
94 Travers et al. (2009) demonstrated increasing water temperature from 17°C to 18°C significantly
95 increased *Vibrio harveyi* associated mortalities in two year old *H. tuberculata* from 0 to ~80%
96 respectively. Blacklip abalone (*Haliotis rubra*) held at elevated water temperatures (21°C or 24°C)
97 for seven days had significantly decreased antibacterial activity (Dang et al. 2012). Reduced
98 antibacterial activity at higher water temperatures may signify a stress induced exhaustion of this
99 aspect of the *Haliotis* spp. immune system (Dang et al. 2012). Vibriosis outbreaks may therefore be
100 a consequence of bacteria exploiting the compromised health of *Haliotis* spp. at elevated water
101 temperatures (Hooper et al. 2007, Lange et al. 2014).

102
103 *Haliotis* spp. gills are the primary organ impacted by infections from different pathogens and gill
104 damage can provide an entry portal for bacteria (Pichon et al. 2013, Hooper et al. 2014b). Mucus
105 which bathes gill epithelium may provide a rich growth medium for bacteria (Sharon & Rosenberg
106 2008). Gills share direct contact with the surrounding environment and consequently, are vulnerable
107 to environmental change (Pichon et al. 2013, Yifan et al. 2015). Gills can therefore provide a visual
108 indicator of oxidative stress and/or inflammation occurring within *Haliotis* spp. (Day et al. 2010,
109 Harris et al. 1998, Hooper et al. 2014b). Elevated water temperature may therefore, be favourable
110 for bacterial infiltration into *Haliotis* spp. gills. Infiltration of *Haliotis* spp. gills by bacteria may
111 also be encouraged by structural damage resulting from by oxidative stress (Pichon et al. 2013,
112 Hooper et al. 2014b). Oxidative gill stress, induced by elevated water temperatures can be
113 visualised by histopathology and has been described for different marine fish species (Madeira et al.
114 2014, Yifan et al. 2015). Japanese flounder (*Paralichthys olivaceus*) gills illustrated serious damage
115 at an elevated water temperature of 32°C and were more sensitive to thermal stress than the other

116 assessed tissue sections (Yifan et al. 2015). When water temperatures exceeded 28°C, gills of
117 gilthead seabream (*Sparus aurata*) (Madeira et al. 2014) contained structural damage including
118 epithelial lifting, oedema and convoluted lamellae (Madeira et al. 2014). Examining abalone gills is
119 therefore a strategy that offers high potential to reveal the processes occurring near their upper
120 thermal limit.

121

122 Histopathology has been used to describe how environmental stressors such as hypoxia and
123 hyperoxia (Harris et al. 1998), anaesthesia and movement (Hooper et al. 2014a), water pollutants
124 (Harris et al. 1998) and pH changes (Harris et al. 1999a) may affect the health of *Haliotis* spp.. No
125 studies involve histopathological assessment of *H. laevisgata* gills maintained at elevated water
126 temperatures long-term are currently available. Hooper et al. (2014b) and Day et al. (2010) assessed
127 the histopathological response of hybrid tiger abalone (*H. laevisgata* x *H. rubra*) gills with short
128 term exposure (seven days) to an elevated water temperature of 26°C. Results from short-term heat
129 exposure studies do not accurately represent physiological responses of *Haliotis* spp. to chronic
130 thermal stress. Long-term heat exposure studies involving histopathology provide a better
131 understanding of *H. laevisgata* responses to conditions experienced on farm during a summer
132 mortality event and allow biomarkers of thermal stress to be identified. Identificaton of biomarkers
133 for thermal stress in *Haliotis* spp. is increasingly important as sea water temperatures are expected
134 to rise with global climate change (Shiel et al. 2017). Histopathology is a practical diagnostic tool
135 that generally relies on qualitative descriptions (Costa 2018). Semi-quantitative histopathological
136 scoring protocols have been developed for freshwater (Bernet et al. 1999) and marine fish (Mitchell
137 et al. 2011). To our knowledge, there is no standardised, quantitative scoring protocol for *H.*
138 *laevisgata* gill histopathology. Using quantitative histopathological analyses may help define
139 significant relationships between *H. laevisgata* lesions and elevated water temperatures. Our study
140 used a semi-quantitative analysis to determine histopathological changes in *H. laevisgata* gills in
141 response to long-term elevated water temperatures. In addition, we proposed a scoring protocol

142 adapted from Bernet et al. (1999), which can be used to assess the histopathological response of *H.*
143 *laevigata* to thermal stress. This protocol provides a flexible template which can be further adapted
144 for histopathological scoring of the gills belonging to any *Haliotis* spp. amid environmental
145 stressors beyond elevated water temperatures.

146

147 **2. MATERIALS AND METHODS**

148

149 **2.1. Experimental animals**

150

151 Experimental *H. laevigata* were used from temperature trials described by Buss et al. (2017).
152 *Haliotis laevigata* were purchased from Pure Australian Abalone (Boston Point, Port Lincoln,
153 South Australia) and held in flow-through systems at the South Australian Research and
154 Development Institute Aquatic Sciences Centre (West Beach, Adelaide, South Australia). Ten
155 individuals were randomly distributed into three replicate tanks (n = 60) which were then subject to
156 either a control (22°C) or elevated water temperature (25°C) treatment. One week after stocking,
157 water temperature for all treatment tanks was increased from the initial temperature of 15°C by
158 ~0.6°C every second day until 22.0°C (30 days). Water temperature for the elevated water
159 temperature treatment group was then further increased by ~1.0°C every second day until 25.0°C
160 (35 days). Water temperature for the control and elevated water temperature treatment groups were
161 maintained for 17 and 12 additional days, respectively, resulting in a total trial period of 47 days.
162 *Haliotis laevigata* were fed a commercial diet from Eyre Peninsula Aquafeeds (Lonsdale, South
163 Australia) to excess (0.6% body weight day⁻¹). Any mortalities were removed and replaced with
164 unmarked similar-sized *H. laevigata* to maintain stocking density within the trial of Buss et al.
165 (2017) and were not sampled for this experiment. After 47 days, two *H. laevigata* from each tank (n
166 =12) were euthanised and a portion of the left gill was placed into separate histology cassettes in
167 seawater-buffered formalin for >24 h and stored in 70% ethanol solution at room temperature.

168 Fixed tissue samples were dehydrated through an ethanol series to histolene, embedded in paraffin
169 wax and sectioned at 5 µm using a Leica RM 2235 rotary microtome (Leica Microsystems GmbH,
170 Wetzlar, Germany). Sections were then floated onto Objektträger microscope slides (90-degree
171 ground edges, twin frosted, ProSciTech Pty Ltd, Kirwan, QLD, Australia.) and dried before
172 staining.

173

174 **2.2. Histopathology**

175

176 Deparaffinised *H. laevigata* gill tissue sections were stained using haematoxylin and eosin and
177 viewed using light microscopy. Two histopathological *H. laevigata* sections were excluded from
178 analysis due to poor staining resulting in a total sample size of five slides each for the control and
179 elevated water temperature treatment groups. All ten slides were scanned using a Hamamatsu
180 NanoZoomer S360 Digital slide scanner 2.0HT and viewed using NDP.view2 software
181 (NanoZoomer Digital Pathology, Hamamatsu Photonics K.K., Iwata City, Japan). *Haliotis*
182 *laevigata* gill leaflets were assessed from the side of the central gill axis (rachis) containing the
183 greatest number of intact leaflets (Fig. 1). Starting at the base of the central gill axis, every second
184 leaflet was assessed (n = 15 gill leaflets). Any gill leaflet <900 µm in length or lacking well defined
185 v-shaped skeletal rods was excluded from examination. Leaflets containing significant artefacts
186 were ignored where possible. Descriptions of *H. laevigata* gill lesions used in histopathological
187 scoring are in Table 1.

188

189 2.2.1 Hemocyte descriptions.

190

191 *Haliotis laevigata* hemocytes were viewed histopathologically using the NDP.view2 software and
192 classified by diameter, nucleus-cytoplasm ratio and nucleus size (Table 4). Hemocyte types were

193 given putative identifications based on previous descriptions of *Haliotis* sp. cell types (Table 4)
194 (Elston 1983, Ottaviani 2011, De Vico and Carella 2012, Pila et al. 2016).

195

196 2.2.2 Scoring

197

198 Histopathological lesions for *H. laevigata* were classified using an adapted version of the protocol
199 proposed by Bernet et al. (1999). To do this, we modified the protocol of Bernet et a. (1999) by
200 assigning reaction patterns, lesions and pathological importance factors which were specific to the
201 morphology and histopathology of *H. laevigata*. Each *H. laevigata* histopathological gill lesion
202 was categorised into one of three different reaction patterns: (1) epithelial, (2) circulatory or (3)
203 inflammatory. Epithelial reaction patterns were lesions leading to an alteration in *H. laevigata*
204 epithelium structure surrounding the hemolymph channel. The circulatory reaction pattern included
205 pathological lesions resulting from changes to *H. laevigata* tissue or hemolymph (Table 1) (Bernet
206 et al. 1999). Inflammation reaction patterns included sites of hemocyte infiltration. Specific
207 histopathological gill lesions for each reaction pattern are described in Table 2.

208

209 *Haliotis laevigata* histopathological gill lesions were assigned pathological importance factors
210 between 1-3 (Bernet et al. 1999) (Table 1). Pathological importance factors were based on the
211 degree of negative impact to the organ and apparent capacity for the lesion to be resolved (Bernet et
212 al. 1999) (Table 1).

213 1 = minor pathological importance: limited impact on organ function and lesion expected to be
214 resolved with improvements to water quality.

215 2 = moderate pathological importance: moderate impact on organ function and in most cases, can
216 expected to be resolved if water quality is improved.

217 3 = substantial pathological importance: total loss of organ function and lesion apparently unable to
218 be resolved.

219

220 *Haliotis laevis* gill leaflets were allocated scores of 1 for lesion presence or 0 for lesion absence.

221 The term, lesion prevalence, was used to define lesion occurrence within each *H. laevis* gill

222 assessed (Bush et al. 1997). Lesion prevalence was then calculated as the percentage of leaflets

223 containing that lesion (Bernet et al. 1999) (*equation 1*):

224

225 *Leaflet lesion prevalence* = (number of leaflets with lesion/15) × 100 [equation 1]

226

227 Each *H. laevis* gill leaflet was scored between 0-5, based on lesion prevalence. Lesions were

228 described as minor, moderate or extensive (Table 3). An alteration index (I_a) for each lesion was

229 then calculated (Bernet et al. 1999) (*equation 2*):

230

231 $I_a = a_x \times w_x$ [equation 2]

232

233 where a_x represents the lesion score and w_x represents the corresponding importance factor. A

234 reaction index (I_r) for each reaction pattern was then calculated as the sum of the alteration indices

235 for that pattern (Bernet et al. 1999) (*equation 3*):

236

237 $I_r = \sum(a_x \times w_x)$ [equation 3]

238

239 A gill index (I_g) for the gill was calculated as the sum of each reaction index (Bernet et al. 1999)

240 (*equation 4*):

241

242 $I_g = \sum(I_r)_x$ [equation 4]

243

244 2.3 Statistical analyses

245

246 Data for leaflet lesion prevalences along with alteration, reaction and gill indices are presented as
247 mean \pm standard deviation. *Haliotis laevigata* gill index, lesion prevalences and alteration indices
248 were tested for normality using the Shapiro-Wilk test (n = 10). Equality of variance based on the
249 means was tested using Levene's test of homogeneity. Total gill and epithelial reaction pattern
250 indices were log transformed while inflammation and circulatory reaction pattern indices were
251 square root transformed. Lesion prevalence (where relevant) and alteration indices for epithelial
252 lifting and necrosis were square root transformed. Transformations were performed to allow indices
253 to meet the assumptions for an independent sample t-test. An independent sample t-test was used to
254 compare means between water temperature groups at a significance level of < 0.05 . A non-
255 parametric Mann Whitney U test was used to compare the medians for alteration indices belonging
256 to the epithelial reaction pattern (hypertrophy, focal hyperplasia, goblet cell hyperplasia and
257 atrophy), circulatory reaction pattern (hemolymph channel enlargement, vascular occlusion and
258 vascular congestion) and inflammation reaction pattern (hemocyte infiltration). All statistical
259 analyses were conducted using IBM SPSS version 26 for Apple Mac (IBM SPSS Inc., Chicago IL).

260

261 **3. RESULTS**

262

263 **3.1 Survival**

264 The survival rate for abalone held at 25°C was below 80% while no mortalities occurred in the
265 22°C group.

266

267 **3.2 Histopathological descriptions**

268

269 3.2.1 Lesion descriptions – Epithelial reaction pattern

270

271 The most extensive epithelial reaction patterns (score 5, Table 3, Table 5) across both temperatures
272 included epithelial hypertrophy and focal hyperplasia (Fig. 2). Epithelial lifting at v-shaped skeletal
273 rods (Fig. 2) occurred extensively (score 5) in *H. laevigata* held at 25°C but was only minor (score
274 2) in *H. laevigata* held at 22°C (Table 3, Table 5). Moderate epithelial atrophy and minor goblet
275 cell hyperplasia (Fig. 2) were observed in both water temperature treatments (scores 3-4, Table 3,
276 Table 5). Moderate epithelial necrosis (Fig. 2) was present in both water temperature treatments
277 (score 2-3, Table 3, Table 5). Minor lamellar fusion (Fig. 2) was observed at 25°C (score 1, Table 3,
278 Table 5), however, did not occur in *H. laevigata* held at 22°C (score 0, Table 3, Table 5).

279

280 3.2.2 Lesion descriptions – Circulatory reaction pattern

281

282 Lesions belonging to the circulatory disturbance reaction pattern (Table 1) ranged from minor to
283 moderate (scores 1-4, Table 3, Table 5). Hemolymph channel enlargement (Fig. 2) was moderate
284 (score 4) in the 25°C water temperature treatment while *H. laevigata* held at 22°C only had minor
285 levels of this lesion (score 1, Table 3, Table 5). Haemorrhage and rupture of the hemolymph
286 channel and vascular occlusion (Fig. 2) in *H. laevigata* were minor (scores 1-2 respectively, Table
287 3, Table 5) at both 22°C and 25°C. Vascular congestion (Fig. 2) did not occur in *H. laevigata* held at
288 22°C and was only minor for *H. laevigata* held at 25°C (score 1, Table 3, Table 5).

289

290 3.2.3 Lesion descriptions – Inflammation reaction pattern

291

292 Hemocyte infiltration (Fig. 2), in the inflammation reaction pattern (Table 1), was minor (score 1)
293 in the 22°C temperature group and moderate (score 4) in abalone held at 25°C (Table 3, Table 5).

294

295 3.2.4 Hemocyte descriptions

296

297 Three different immune-responsive cells were observed in *H. laevigata* gills: two circulating
298 hemocytes (small hyalinocytes, larger hyalinocytes), and/or granulocytes (non-circulating, fixed
299 granular cells) (Table 5). Small hyalinocytes appeared undifferentiated and blast-like with a smaller
300 diameter, when compared to larger hyalinocytes and a large nucleus-cytoplasm ratio (Table 5).
301 Small hyalinocytes were most prevalent in hemolymph channels, within *H. laevigata* gills. Larger
302 hyalinocytes had a smaller nucleus-cytoplasm ratio when compared to small hyalinocytes and
303 granulocytes. Granulocytes were the least observed cell type and were distinguished by a large
304 diameter, low nucleus-cytoplasm ratio, the presence of granules and in some cases, pseudopods
305 (Table 5).

306

307 One *H. laevigata* gill from the 22°C water temperature group contained larger hemocytes than any
308 other *H. laevigata* gill assessed. Large hemocytes were only present near a substantial area of
309 epithelial loss at the tip of a v-shaped skeletal rod (Fig. 3). Cells contained enlarged nuclei, a high
310 nucleus-to-cytoplasm ratio (Table 5), were often pleomorphic, with mitotic figures and in some
311 cases, two dividing nuclei (Table 5).

312

313 **3.3 Histopathological scoring**

314

315 Epithelial reaction pattern indices were 28.00 ± 8.60 and 41.00 ± 12.94 for *H. laevigata* exposed to
316 22°C and 25°C respectively (Fig. 4, Table 5). Differences between epithelial reaction pattern
317 indices at 22°C and 25°C were not significant ($p = 0.087$, Table 5). Water temperature had no effect
318 on the prevalence of focal hyperplasia ($p = 0.690$), goblet cell hyperplasia ($p = 0.080$), lamellar
319 fusion ($p = 0.310$), atrophy ($p = 0.715$) or necrosis ($p = 0.548$) in *H. laevigata* (Table 5). At 22°C,
320 epithelial hypertrophy occurred in $97.33 \pm 5.96\%$ of assessed leaflets, which was similar to *H.*
321 *laevigata* held at 25°C ($80.00 \pm 18.86\%$) ($p = 0.095$, Table 5). The prevalence of epithelial lifting
322 was significantly greater in *H. laevigata* held at 25°C ($93.33 \pm 11.55\%$) than for *H. laevigata* held at

323 22°C ($34.67 \pm 28.83\%$) ($p = 0.008$, Table 5).

324

325 The circulatory reaction pattern index was greater for *H. laevigata* held at 25°C (13.60 ± 8.99) than
326 for *H. laevigata* at 22°C (2.8 ± 2.2) ($p = 0.039$, Fig 4, Table 5). Water temperature had no effect on
327 the occurrence of hemolymph channel rupture ($p = 0.069$), vascular occlusion ($p = 0.151$) or
328 vascular congestion ($p = 0.310$) in *H. laevigata* ($p > 0.05$, Table 5). Hemolymph channel
329 enlargement was significantly more common in *H. laevigata* exposed to 25°C ($74.67 \pm 40.66\%$)
330 than *H. laevigata* exposed to 22°C (8.00 ± 8.69) ($p = 0.032$, Table 5).

331

332 Inflammatory reaction pattern indices were 0.60 ± 0.50 and 4.20 ± 2.68 for *H. laevigata* exposed to
333 22°C and 25°C respectively (Fig. 4, Table 5). Differences between inflammatory reaction pattern
334 indices at 22°C and 25°C were not significant ($p = 0.095$, Table 5). Water temperature had no
335 significant effect on the occurrence of hemocyte infiltration in *H. laevigata* ($p > 0.05$, Table 5).

336

337 The overall gill index for *H. laevigata* held at 22°C was 31.40 ± 9.80 , which was significantly
338 lower than for *H. laevigata* held at 25°C (58.80 ± 20.78) ($p = 0.026$, Table 5).

339

340 **4. DISCUSSION**

341

342 Quantitative assessment of histopathological slides can be complicated when little reference
343 information is available. Prior studies used different semi-quantitative approaches to score
344 histopathological lesions in *H. laevigata* (Harris et al. 1999a, Hooper et al. 2014a, b). Hooper et al
345 (2014a) used semi-quantitative scales for assessing hemocyte prevalence and intensity of
346 eosinophilia in the papilla of the left kidney following anaesthesia and movement of
347 *H. laevigata* x *H. rubra*. A similar semi-quantitative scoring protocol was used to quantify the
348 intensity of eosinophilia in gills and oedema and hemocyte infiltration in the digestive gland of

349 *H. laevigata* x *H. rubra* after acute thermal stress (Hooper et al. 2014b). Harris et al. (1998a) used a
350 scale system (1-3) to categorise lesions in the gill and left kidney of *H. laevigata* exposed to high
351 ammonia, nitrate and low dissolved oxygen rates. Bernet et al. (1999) developed a protocol to
352 assess histopathological responses of freshwater fish to waterborne pollutants. Semi-quantitative
353 scores are created by consolidating large amounts of observational data into numerical semi-
354 quantitative scores. Loss of data and information during this process can therefore lead to
355 misinterpretation of histopathological lesions and the associated relationship between lesion
356 presence with a cause (Wolf, 2018). To address this limitation, our semi-quantitative scoring system
357 provides individual histopathological descriptions and summary values which are specific to
358 morphology and histopathology observations of *H. laevigata*. Together, the use of histopathological
359 descriptors and summary values offers a stronger approach than the use of either alone. Our adapted
360 protocol can be used as a standardised method for scoring histopathological changes in *H. laevigata*
361 gills amid environmental stress to complement histopathological descriptions. Our histopathological
362 scoring protocol also provides a template which can be further adapted to different species using
363 additional or alternative histopathological changes.

364

365 We are the first to assess histopathological responses of *H. laevigata* to long-term elevated water
366 temperatures. We selected *H. laevigata* which survived the temperature trial; relative scores and
367 lesion prevalences determined in this study therefore denote lesion characteristics associated with
368 either *H. laevigata* survival or progression towards mortality. Gill index describes the number of
369 gill lesions, with a higher index indicating a higher number of lesions. *Halibut laevigata* held in
370 warmer water had higher gill indices than *H. laevigata* held in cooler water, indicating chronic,
371 long-term temperature stress results in increased lesion prevalence. Gill indices, using our scoring
372 protocol may therefore be a reliable quantitative method to identify summer mortality in *H.*
373 *laevigata*.

374

375 Greater epithelial lifting occurred in *H. laevisgata* held at elevated water temperatures when
376 compared to the control group (Table 4). In some cases, the subsequent epithelial loss following
377 epithelial lifting led to complete fusion of the epithelium lining adjacent leaflets (Fig. 2, Table 4).
378 Hooper et al. (2014b) found greater epithelial loss in the gills of acute heat stressed
379 *H. laevisgata* x *H. rubra* compared to controls. The only published description of persistent
380 epithelial lifting in *H. laevisgata* without overt epithelial loss was reported in *H. laevisgata* exposed
381 to sub-lethal concentrations of nitrite (Harris et al. 1998). Epithelial lifting has been described in
382 other molluscs and is a major histopathological symptom of oyster oedema disease, an
383 economically troubling disease affecting the pearl oyster (*Pinctada maxima*) (Jones et al. 2010,
384 Goncalves et al. 2017). The aetiology of oyster oedema disease remains unknown, however, it is
385 typically accompanied by tissue oedema and lifting of intestinal and stomach epithelium (Jones et
386 al. 2010, Goncalves et al. 2017).

387

388 Epithelial lifting has been observed in the gills of various fish species exposed to elevated water
389 temperatures (Madeira et al. 2014, Yifan et al. 2015), waterborne pollutants (Mallat 1985, Zhihao et
390 al. 2012, Hassaninezhad et al. 2014, Lujic et al. 2015) and both stressors simultaneously (Salazar-
391 Lugo et al. 2011). Mallat (1985) reviewed fish gill histopathological alterations and suggested that
392 epithelial lifting was the most commonly reported lesion and may result from an infiltration of fluid
393 into the interlamellar space. Epithelial lifting is common in many types of epithelial cell
394 degeneration and may also serve as an indicator of early sloughing or loss of epithelium. The
395 deleterious effects of waterborne pollutants, specifically transition metals, may be exacerbated by
396 elevated water temperatures (Sokolova 2004, Cherkasov et al. 2007). Epithelial lifting in *H.*
397 *laevisgata* gills during periods of elevated temperature may therefore be a consequence of increased
398 sensitivity to pollutants at elevated water temperature rather than thermal stress alone. This
399 suggestion cannot be confirmed as the concentration of waterborne pollutants were not measured by

400 Buss et al. (2017), however, an association of this lesion with elevated water temperature allows
401 epithelial lifting to be used as a histopathological biomarker of thermal stress.

402

403 Hemolymph channel enlargement was more prevalent in *H. laevigata* held in warmer water
404 temperature (Table 4) and potentially occurred to accommodate for a greater quantity of hemocytes
405 and hemolymph volume similar to vessel dilation in vertebrates held in warm conditions.

406 Hemolymph channel enlargement may be a progressive alteration which, possibly due to vascular
407 wall damage, can gradually result in a focal distention of the hemolymph channel. Consequently,
408 hemolymph channel enlargement may act as a precursor for vascular occlusion which may be
409 associated with a reduction in haemolymph channel function following severe thermal stress. Of the
410 three reaction patterns analysed, only the circulatory reaction pattern index increased with elevated
411 water temperature suggesting hemolymph channel structure is more affected by thermal stress than
412 epithelial or inflammatory reaction patterns.

413

414 Hemocyte infiltration in *H. laevigata* gills was observed but did not differ between water
415 temperature treatments, which may reflect the ability of this lesion to be resolved if water
416 conditions improve. Day et al. (2010) described hemocyte infiltration in the gills of *H. laevigata* x
417 *H. rubra* held at 26°C for seven days however, these results were not quantified. Following this,
418 Hooper et al. (2014b) quantitatively demonstrated greater infiltration in the digestive gland of
419 hybrid *H. laevigata* x *H. rubra* held at 26°C for seven days. No hemocyte infiltration in the gills of
420 *H. laevigata* x *H. rubra* was reported by Hooper et al. (2014b).

421

422 Substantial epithelial necrosis in the gills of hybrid *H. laevigata* x *H. rubra* held at an elevated
423 water temperature of 26°C has been described (Day et al. 2010, Hooper et al. 2014b). Similarly,
424 severe epithelial necrosis was observed in *P. olivaceus* gills with acute exposure (24 h) to an
425 elevated water temperature of 32°C (Yifan et al. 2015). Necrosis in the tissue of aquatic organisms,

426 such as finfish and molluscs, can indicate oxidative stress (Lushchak 2011). An accumulation of
427 ROS can result in damage to DNA and proteins as well as the oxidation of polyunsaturated fatty
428 acids, which can all manifest as cell necrosis (Abele & Puntarulo 2004, Lushchak 2011). We
429 showed elevated water temperature can increase necrosis in *H. laevigata* gills, however, the
430 difference was not statistically significant to *H. laevigata* gills held in cooler water (Table 4). Only
431 *H. laevigata* which survived the water temperature trial were assessed and tissue necrosis may have
432 been more apparent in dead *H. laevigata*. In live *H. laevigata*, however, necrosis was not a reliable
433 indicator of summer mortality.

434

435 In addition to circulating hemocytes, fixed granular cells were seen at low prevalence within *H.*
436 *laevigata* gill tissue, fitting prior descriptions of molluscan granulocytes (De Vico & Carella 2012).
437 There are inconsistent reports of granulocyte cells in *Haliotis* spp.. Granulocytes have been
438 described in the hemolymph of *H. diversicolor* (Hong et al. 2019) and Donkey's ear abalone
439 (*Haliotis asinina*) (Sahaphong et al. 2001), but were absent in the disk abalone (*Haliotis discus*
440 *discus*) (Donaghy et al. 2010). Travers et al. (2008b) failed to distinguish granulocytes in *H.*
441 *tuberculata* using either flow cytometry, phase contrast microscopy or transmission electron
442 microscopy, despite being visible histopathologically. Pichon et al. (2013) later identified
443 granulocytes in primary gill cultures of *H. tuberculata* using phase contrast microscopy. An
444 alternative suggestion is that gill granulocytes may resemble the hemocyanin synthesising
445 rhogocytes previously described in the mantle tissue of *H. laevigata* (Sairi et al. 2015). Sairi et al.
446 (2015) described rhogocytes as having an irregular and ovoid shape ranging in size from 10 to
447 30µm. Descriptions of rhogocytes in molluscs vary and therefore, describing the non-circulating,
448 fixed granular cells observed in this study as rhogocytes is putative.

449

450 One *H. laevigata* held at 22°C had a proliferation of larger, multinucleate hemocytes which were
451 often pleomorphic and illustrated a greater nucleus-to-cytoplasm ratio (Table 5, Fig. 33). These

452 novel cells are undescribed in the literature. A known consequence of stress in *Haliotis* spp. is a
453 decrease in the quantity of hemocytes (hemocytopenia) within hemolymph fluid (Cheng et al.
454 2004b, Day et al. 2010). A proposed explanation for hemocytopenia following environmental stress
455 is the migration and infiltration of hemocytes to areas damaged by physical affliction or oxidative
456 stress (Malham et al. 2003, Day et al. 2010), which may deplete hemocyte reserves. The area
457 responsible for hemocyte production (haematopoiesis) in *Haliotis* spp. is yet to be identified (Day et
458 al. 2010) and very little is understood about haematopoiesis in invertebrates (Pila et al. 2016).
459 Considering the close proximity of the cells in this study to a large infiltration of cells in a v-shaped
460 skeletal rod (Fig. 3), it is possible that they represent a region of haematopoiesis in response to
461 hemocyte loss or migration to a lesion. An alternative suggestion is that these cells may be
462 neoplastic. There are two important neoplastic lesions described for bivalve molluscs: disseminated
463 neoplasia (DN) and gonadal neoplasia (Aguilera 2017, Barber 2004, Metzger et al. 2016).
464 Disseminated neoplasia is defined by frequent mitosis of anaplastic cells with enlarged nuclei and
465 considerably greater nucleus-to-cytoplasm ratios. Disseminated neoplasia has commonly been
466 identified in the circulatory systems and hemolymph channels of bivalve molluscs (Aguilera 2017,
467 Barber 2004, Carballal et al. 2013, Ciocan & Sunila 2005, Le Grand et al. 2010, Metzger et al.
468 2016). However, neoplasia has not been previously described in *Haliotis* spp.. The only tumours
469 described in gastropoda are benign lesions in land snails (Tascedda & Ottaviani 2014). In bivalves,
470 DN can be transmitted from diseased to healthy individuals (Barber 2004, Carballal et al. 2013,
471 Ciocan & Sunila 2005) and infectious behaviour may be heightened by environmental stress
472 (Barber 2004), although no direct association with thermal stress has been identified (Carballal et
473 al. 2013). Common diagnoses of DN use histopathology of the diseased region and/or direct
474 examination of the hemolymph, referred to as hemocytology (Barber 2004). These novel cells were
475 a secondary finding and histopathology was the only diagnostic tool available at the time of
476 discovery. Observed cells, however, did not exceed the size of normal replicating cells, were
477 restricted to one region and were absent from adjacent folia which are characteristics not typical of

478 DN. Ideally, other diagnostic tools such as hemocytology would be used to provide a confirmatory
479 identification of this cell population.

480

481 This study relied on gill histopathology slides from *H. laevisgata* used in previous water temperature
482 trials and was limited by a small sample size. Limited samples within each water treatment group
483 should be considered when using these results to draw conclusions about the histopathological
484 response of larger *H. laevisgata* cohorts to elevated water temperature. Furthermore, the potential for
485 some lesions to be artefactual or a result of handling *H. laevisgata* gills during sample preparation
486 needs to be acknowledged. Future studies regarding thermal stress in *H. laevisgata* should consider a
487 concurrent analysis of histopathology with biomarkers for oxidative stress, allowing more accurate
488 conclusionsconclusions to be made about the origin of lesions. Gene expression paired with
489 quantitative histopathology (such as our scoring protocol) may also help increase understanding of
490 the genes associated with resistance to lesions induced by thermal stress. This is increasingly
491 important as the potential for selective breeding and genetic improvement of *H. laevisgata* as means
492 of combating summer mortality is recognised. Histopathological assessment in all areas of *Haliotis*
493 spp. research will be greatly enhanced through the use of the standardised semi-quantitative scoring
494 protocol proposed in this study.

495

496 **5. CONCLUSION**

497

498 We adapted and created a standardised method to semi-quantitatively score the histopathological
499 response of *H. laevisgata* to environmental stress. This protocol was successfully used to assess the
500 histopathological response of *H. laevisgata* gills to long-term elevated water temperatures. Overall
501 gill index was higher for *H. laevisgata* held at 25°C than at 22°C suggesting *H. laevisgata* gills
502 experience pathological changes with long-term exposure to elevated water temperatures. These
503 pathological changes may represent defence mechanisms associated with survival or characteristics

504 which are progressive towards mortality. *Haliotis laevis* held at 25°C had a significantly higher
505 circulatory reaction pattern index than *H. laevis* at 22°C therefore, hemolymph channels may be
506 more vulnerable to thermal stress than reaction patterns associated with epithelium or inflammation.
507 Increased prevalence of epithelial lifting at 25°C may allow this lesion to be used as a
508 histopathological biomarker for thermal stress in *H. laevis*. An area of apparent hemocyte
509 proliferation was identified in the tissue surrounding the v-shaped skeletal rod of one leaflet. These
510 cells were characterised by the presence of enlarged nuclei, a greater nucleus-to-cytoplasm ratio and
511 in some cases, mitotic figures, which may represent a region of hematopoiesis in response to
512 excessive loss of hemocytes or migration to a lesion. Given that no specific site has been found for
513 hematopoiesis in *H. laevis*, the presence of proliferating cells near a lesion, with evidence of
514 continued cells loss is of interest and warrants future research.

515

516 *Acknowledgements.* This research forms part of a larger South Australian Government funded Food
517 Focus Program project entitled, “Thriving Abalone” and was supported by the South Australian
518 Research and Development Institute (SARDI) and Marine Innovation Southern Australia (MISA),
519 the Australian Abalone Growers’ Association, Aqua Feeds Australia Pty. Ltd. and Eyre Peninsula
520 Aquafeed Pty. Ltd. (EPA). We would like to thank Mr Joel Scanlon of Aqua Feeds Australia Pty.
521 Ltd. and Dr Thomas Coote and Mr Kym Heidenreich of EPA who provided ingredients and helped
522 manufacture the diets. We would also like to thank students from Flinders University and the
523 University of Adelaide for their technical assistance during this study, including Dr Matthew
524 Bansemer, Ms Krishna-Lee Currie, Mrs Elise Schaefer, Dr Georgia Mercer, Dr Hanru Wang, Dr
525 James Forwood, Dr Duong Duong, Dr Thanh Hoang, Mr Ben Crowe, Mr Justin Sellars, Mr Rhys
526 Johnson, Ms Sharni Lans, Mr Robert O’Reilly and Dr Maziidah Ab Rahman.

527

528

LITERATURE CITED

529

- 530 Abdel-Tawwab M, Wafeek M (2014) Influence of water temperature and waterborne cadmium
531 toxicity on growth performance and metallothionein-cadmium distribution in different
532 organs of Nile tilapia, *Oreochromis niloticus* (L.). J Therm Biol 45:157-62.
- 533 Abele D, Puntarulo S (2004) Formation of reactive species and induction of antioxidant defence
534 systems in polar and temperate marine invertebrates and fish. Comp Biochem Physiol A
535 138:405-415.
- 536 Aguilera F (2017) Neoplasia in mollusks: what does it tell us about cancer in humans? – A review. J
537 Genet Disord 1(1):7.
- 538 Barber B (2004) Neoplastic diseases of commercially important bivalves. Aquat Living Resourc
539 17:449-66.
- 540 BDO EconSearch (2019) The economic contribution of aquaculture in the South Australian state
541 and regional economies 2017/18, PIRSA, Adelaide, Australia, viewed 12th April 2020
542 <[https://www.pir.sa.gov.au/ data/assets/pdf file/0008/347543/Aquaculture-Economic-](https://www.pir.sa.gov.au/data/assets/pdf_file/0008/347543/Aquaculture-Economic-Impact-Report-2017-2018.pdf)
543 [Impact-Report-2017-2018.pdf](https://www.pir.sa.gov.au/data/assets/pdf_file/0008/347543/Aquaculture-Economic-Impact-Report-2017-2018.pdf)>
- 544 Bernet D, Schmidt H, Meier W, Burkhardt-Holm P, Wahli T (1999) Histopathology in fish:
545 proposal for a protocol to assess aquatic pollution. J Fish Dis 22:25-34.
- 546 Braid BA, Moore JD, Robbins TT, Hedrick RP, Tjeerdema RS, Friedman CS (2005) Health and
547 survival of red abalone, *Haliotis rufescens*, under varying temperature, food supply, and
548 exposure to the agent of withering syndrome. J Invert Pathol 89(3): 219-231.
- 549 Buss JJ, Harris JO, Currie K, Stone DAJ (2017) Survival and feeding of greenlip abalone (*Haliotis*
550 *laevigata*) in response to a commercially available dietary additive at high water
551 temperature. J Shellfish Res 36:763-70.
- 552 Bush AO, Lafferty KD, Lotz JM, Shostak AW (1997) Parasitology meets ecology on its own
553 terms: Margolis et al. revisited. J Parasitol 83(4): 575-83.

- 554 Carballal M, Iglesias D, Diaz D, Antonio V (2013) Disseminated neoplasia in clams *Venerupis*
555 *aurea* from Galicia (NW Spain): Histopathology, ultrastructure and ploidy of neoplastic
556 cells, and comparison of diagnostic procedures. *J Invert Pathol* 112:16-19.
- 557 Cardinaud M, Dheilily N, Huchette S, Moraga D, Paillard C (2015) The early stages of the immune
558 response of the European abalone *Haliotis tuberculata* to a *Vibrio harveyi* infection. *Dev*
559 *Comp Immunol* 51:287-97.
- 560 Cheng W, Hsiao I, Hsu C, Chen J (2004a) Change in water temperature on the immune response of
561 Taiwan abalone *Haliotis diversicolor supertexta* and its susceptibility to *Vibrio*
562 *parahaemolyticus*. *Fish Shellfish Immunol* 17:235-43.
- 563 Cheng W, Liu C, Cheng S, Chen J (2004b) Effect of dissolved oxygen on the acid-base balance and
564 ion concentration of Taiwan abalone *Haliotis diversicolor supertexta*. *Aquaculture* 231:573-
565 86.
- 566 Cherkasov AS, Grewal S, Sokolova IM (2007) Combined effects of temperature and cadmium
567 exposure on haemocyte apoptosis and cadmium accumulation in the eastern oyster
568 *Crassostrea virginica* (Gmelin). *J Therm Biol* 32:162-70.
- 569 Ciocan C, Sunila I (2005) Disseminated neoplasia in blue mussels, *Mytilus galloprovincialis*, from
570 the Black Sea, Romania. *Mar Pollut Bull* 50:1335-9.
- 571 Costa PM (2018) *The Handbook of Histopathological Practices in Aquatic Environments: Guide to*
572 *Histology for Environmental Toxicology*. Academic Press, United Kingdom.
- 573 Dang VT, Speck P, Benkendorff K (2012) Influence of elevated temperatures on the immune
574 response of abalone, *Haliotis rubra*. *Fish Shellfish Immunol* 32:732-40.
- 575 Day R, Hooper C, Benkendorff K, Slocombe R, Handlinger J (2010) Investigations on the
576 immunology of stressed abalone. FRDC final report 2004/233. Fisheries Research and
577 Development Corporation, Canberra.
- 578 De Vico G, Carella F (2012) Morphological features of the inflammatory response in molluscs. *Res*
579 *Vet Sci* 93:1109-15.

- 580 De Zoysa M, Pushpamali WA, Oh C, Whang I, Kim SJ, Lee J (2008) Transcriptional up regulation
581 of disk abalone (*Haliotis discus discus*) selenium dependent glutathione peroxidase by H₂O₂
582 oxidative stress and *Vibrio alginolyticus* bacterial infection. Fish Shellfish Immunol 25:446-
583 57.
- 584 De Zoysa M, Whang I, Lee Y, Lee S, Lee J (2009) Transcriptional analysis of antioxidant and
585 immune defence genes in disk abalone (*Haliotis discus discus*) during thermal, low-salinity
586 and hypoxic stress. Comp Biochem Physiol B 154:387-95.
- 587 Donaghy L, Hong H, Lambert C, Park H, Shim W.J., Choi K. (2010) First characterisation of the
588 populations and immune-related activities from two edible gastropod species, the disk
589 abalone, *Haliotis discus discus* and the shiny top shell, *Turbo cornutus*. Fish Shellfish
590 Immunol 28: 87-97.
- 591 Elston R (1983) Histopathology of oxygen intoxication in the juvenile red abalone, *Haliotis*
592 *ruescens* Swainson. J Fish Dis 6:101-110.
- 593 Friedman CS, Thomson M, Calvin C, Haaker PL, Hedrick RP (1997) Withering syndrome of the
594 black abalone *Haliotis cracherodii* (Leach): Water temperature, food availability, and
595 parasites as possible causes. J Shellfish Res. 16(2): 403-411.
- 596 Goncalves P, Raftos D, Jones D, Anderson K, Jones B, Snow M (2017) Identifying the cause of
597 Oyster Oedema Disease (OOD) in pearl oysters (*Pinctada maxima*) and developing
598 diagnostic tests for OOD. FRDC final report 2013/002. Fisheries Research and
599 Development Cooperation, Canberra.
- 600 Handlinger J, Carson J, Donachie L, Gabor L, Taylor D (2005). Bacterial infection in farmed
601 Tasmanian abalone: causes, pathology, farm factors and control options. In: Walker PJ,
602 Lester RG, Bondad-Reantaso MG (eds.) Diseases in Asian Aquaculture V. Proceedings of
603 the 5th Symposium on Diseases in Asian Aquaculture. Fish Health Section, Asian Fisheries
604 Society, Manila. pp. 289-299.

605 Harris JO, Maguire GB, Handler J (1998) Effects of exposure of greenlip abalone, *Haliotis*
606 *laevigata* Donovan, to high ammonia, nitrite and low dissolved oxygen concentrations on
607 gill and kidney structure. J Shellfish Res 17:683-87.

608 Harris JO, Maguire G, Edwards S, Hindrum S (1999a) Effect of pH on growth rate, oxygen
609 consumption rate, and histopathology of gill and kidney tissue for juvenile greenlip abalone,
610 *Haliotis laevigata* Donovan and blacklip abalone, *Haliotis rubra* Leach. J Shellfish Res
611 18:611-19.

612 Harris JO, Maguire G, Edwards S, Johns D (1999b) Low dissolved oxygen reduces growth rate and
613 oxygen consumption rate of juvenile greenlip abalone, *Haliotis laevigata* Donovan.
614 Aquaculture 174:265-78.

615 Hassaninezhad L, Safaheih A, Salamat N, Savari S, Majd NE (2014) Assessment of gill
616 pathological responses in the tropical fish yellowfin seabream of Persian Gulf under
617 mercury exposure. Toxicol Rep 1:621-28.

618 Hong H, Donaghy L, Choi K (2019) Flow cytometric characterisation of hemocytes of the abalone
619 *Haliotis diversicolor* (Reeve, 1846) and effects of air exposure stresses on hemocyte
620 parameters. Aquaculture 506:401-409.

621 Hooper C, Day R, Slocombe R, Handler J, Benkendorff K (2007) Stress and immune responses
622 in abalone: Limitations in current knowledge and investigative methods based on other
623 models. Fish Shellfish Immunol 22:363-79.

624 Hooper C, Day R, Slocombe R, Benkendorff K (2014a) Histopathology and haemolymph
625 biochemistry following anaesthesia and movement in farmed Australian abalone (hybrid
626 *Haliotis laevigata* x *Haliotis rubra*). Aquaculture 422:202-10.

627 Hooper C, Day R, Slocombe R, Benkendorff K, Handler J, Goulias J (2014b) Effects of severe
628 heat stress on immune function, biochemistry and histopathology in farmed Australian
629 abalone (hybrid *Haliotis laevigata* x *Haliotis rubra*). Aquaculture 432:26-37.

- 630 Jones JB, Crockford M, Creeper J, Stephens F (2010) Histopathology of oedema in pearl oysters
631 *Pinctada maxima*. Dis Aquat Org 91:61-73.
- 632 Lange B, Currie K-L, Howarth GS, Stone DAJ (2014) Grape seed extract and dried macroalgae,
633 *Ulva lactuca* Linnaeus, improve survival of greenlip abalone, *Haliotis laevigata* Donovan,
634 at high water temperature. Aquaculture 43:348-60.
- 635 Le Grand F, Kraffe E, de Montaudouin X, Villalba A, Marty Y, Soudant P (2010) Prevalence,
636 intensity and aneuploidy patterns of disseminated neoplasia in cockles (*Cerastoderma*
637 *edule*) from Archachon Bay: Seasonal variation and position in sediment. J Invert Pathol
638 104:110-18.
- 639 Lujic J, Matavulj M, Poleksic V, Raskovic B, Marinovic Z, Kostic D, Miljanovic B (2015) Gill
640 reaction to pollutants from the Tamis river in three freshwater fish species, *Esoc lucius* L.
641 1758, *Sander lucioperca* (L. 1758) and *Silurus glanis* L. 1758: A comparative study. Anot
642 Histol 44:128-37.
- 643 Lushchak V (2011) Environmentally induced oxidative stress in aquatic animals. Aquat Toxicol
644 101:13-30.
- 645 Madeira D, Vinagre C, Costa P, Diniz M (2014) Histopathological alterations, physiological limits,
646 and molecular changes of juvenile *Sparus aurata* in response to thermal stress. Mar Ecol
647 Prog Ser 505:253-66.
- 648 Malham SK, Lacoste A, Gelebart F, Cueff A, Poulet SA (2003) Evidence for a direct link between
649 stress and immunity in the mollusc *Haliotis tuberculata*. J Exp Zool 295A:136-144.
- 650 Mallat J (1985) Fish gill structural changes induced by toxicants and other irritants: A statistical
651 review. Can J Fish Aquat Sci 42:630-48.
- 652 Metzger MJ, Villalba A, Carballal MJ, Iglesias D, Sherry J, Reinisch C, Muttray AF, Baldwin SA,
653 Goff SP (2016) Widespread transmission of independent cancer lineages within multiple
654 bivalve lineages. Nature 534(7609): 705-709.

- 655 Mitchell SO, Baxter EJ, Holland C, Rodger HD (2012) Development of a novel histopathological
656 assessment of gill health during a longitudinal study in marine-farmed Atlantic salmon
657 (*Salmo salar*). *Aquacult Int* 20:813-25.
- 658 Nicolas JL, Basuyaux O, Mazurie J, Thebault A (2002) *Vibrio carcharie*, a pathogen of the abalone
659 *Haliotis tuberculata*. *Dis Aquat Organ* 50:35-43.
- 660 Ottaviani E (2011) Immunocyte: the invertebrate counterpart of the vertebrate macrophage. *Invert*
661 *Surviv J* 8:1-4.
- 662 Pichon D, Cudennec B, Huchette S, Djediat C, Renault T, Paillard C, Auzoux-Bordenave S (2013)
663 Characterisation of abalone *Haliotis tuberculata*-*Vibrio harveyi* interactions in gill primary
664 cultures. *Cytotechnology* 65:759-72.
- 665 Pila EA, Sullivan JT, Wu XZ, Fang J, Rudko SP, Gordy MA, Hanington PC (2016) Haematopoiesis
666 in molluscs: a review of hemocyte development and function in gastropods, cephalopods
667 and bivalves. *Dev Comp Immunol* 58:119-28.
- 668 Sairi F, Valtchev P, Gomes V.G., Dehghani F (2015) Distribution and characterisation of rhogocyte
669 cell types in the mantle tissue of *Haliotis laevigata*. *Mar Biotechnol* 17:168-179.
- 670 Sahaphong S, Linthong V, Wanichanon C, Reingrojpitak S (2001) Morphofunctional study of the
671 hemocytes of *Haliotis asinina*. *J Shellfish Res* 20(2):711-716.
- 672 Salazar-Lugo R, Mata C, Oliveros A, Rojas LM, Lemus M, Rojas-Villaruel E (2011)
673 Histopathological changes in gill, liver and kidney of neotropical fish *Colossoma*
674 *macropomum* exposed to paraquat at different temperatures. *Environmen Toxicol*
675 *Pharmacol* 31:490-5.
- 676 Sharon G, Rosenberg E (2008) Bacteria growth on coral mucus. *Curr Microbiol* 56:481-8
- 677 Shiel BP, Cooke IR, Hall NE, Robinson NA, Srugnell JM (2018) Summer mortality in molluscs:
678 the genetic basis for resilience and susceptibility. In: Hermes S and Dominik S (eds)
679 *Breeding Focus 2018 – Reducing Heat Stress*. Animal Genetics and Breeding Unit,
680 University of New England, NSW, Australia, p 59-79.

681 Shiel BP, Cooke IR, Hall NE, Robinson NA, Strugnell JM (2020) Gene expression differences
682 between abalone that are susceptible and resilient to a simulated heat wave event.
683 *Aquaculture* 526:735317.

684 Shiel BP, Hall NE, Cooke IR, Robinson NA, Strugnell JM (2017) Epipodial tentacle gene
685 expression and predetermined resilience to summer mortality in the commercially important
686 greenlip abalone, *Haliotis laevis*. *Mar Biotechnol* 19(2): 191-205.

687 Sokolova IM (2004) Cadmium effects on mitochondrial function are enhanced by elevated
688 temperatures in marine poikilotherm, *Crassostrea virginica* Gmelin (Bivalva: Ostreidae). *J*
689 *Exp Biol* 207:2639-48.

690 Stone DAJ, Harris JO, Wang H, Mercer GJ, Schaefer EN (2013) Dietary protein level and water
691 temperature interactions for greenlip abalone *Haliotis laevis*. *J Shellfish Res* 32:119-30.

692 Stone DAJ, Bansemer MS, Currie K-L, Saunders L, Harris JO (2016) Increased dietary protein
693 improves the commercial production of hybrid abalone (*Haliotis laevis* x *Haliotis rubra*).
694 *J Shellfish Res* 35:695-701.

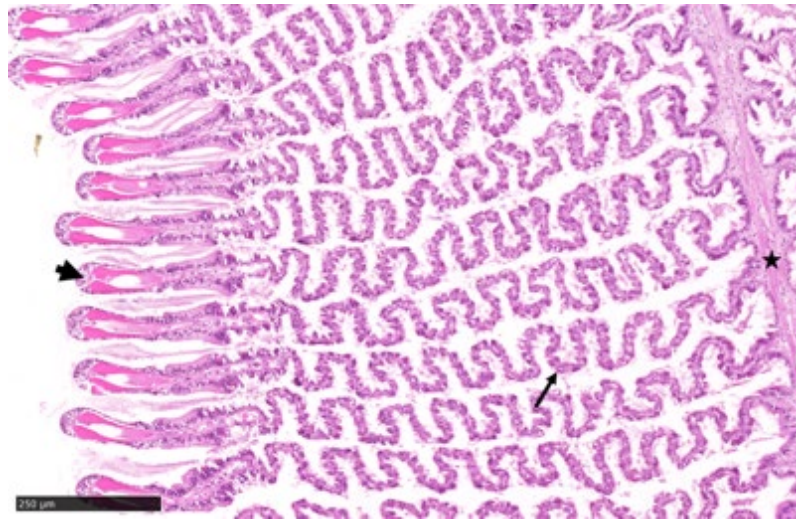
695 Tascetta F, Ottaviani E (2014) Tumors in invertebrates. *Invert Surviv J* 11:197-203.

696 Travers M, Goic N, Huchette S, Koken M, Paillard C (2008a) Summer immune depression
697 associated with increased susceptibility of the European abalone, *Haliotis tuberculata* to
698 *Vibrio harveyi* infection. *Fish Shellfish Immunol* 25:800-808.

699 Travers M, Mirella da Silva P, Le Goic N, Marie D, Donval A, Huchette S, Koken M, Paillard C
700 (2008b) Morphologic, cytometric and functional characterisation of abalone (*Haliotis*
701 *tuberculata*) haemocytes. *Fish Shellfish Immunol* 24:400-411.

702 Travers M, Basuyaux O, Goic N, Huchette S, Nicolas J, Koken M, Paillard C (2009) Influence of
703 temperature and spawning effort on *Haliotis tuberculata* mortalities caused by *Vibrio*
704 *harveyi*: an example of emerging vibriosis linked to global warming. *Global Change Biol*
705 15:1365-76.

- 706 Vandeeper M (2006) Preventing summer mortality of abalone in aquaculture systems by
707 understanding interactions between nutrition and water temperature. SARDI Aquatic
708 Sciences Report RD02/0035-2. South Australian Research and Development Institute,
709 Adelaide.
- 710 Vosloo D, Vosloo A (2010) Response of cold-acclimated, farmed South African abalone (*Haliotis*
711 *midae*) to short-term and long-term changes in temperature. *J Thermal Biol* 35:317-23.
- 712 Vosloo D, Van Rensburg L, Vosloo A (2013) Oxidative stress in abalone: The role of temperature,
713 oxygen and L-proline supplementation. *Aquaculture* 416:265-71.
- 714 Wolf JC (2018) Comparing apples and oranges and pears and kumquats: The misuse of index
715 systems for processing histopathology data in fish toxicological bioassays. *Environ Toxicol*
716 *Chem* 37(6):1688-95.
- 717 Yifan L, Daoyuan M, Zhizong X, Shihong X, Yanfeg W, Yufu W, Yongshuang X, Zongcheng S,
718 Zhaojun T, Qinghua L, Jun L (2015) Histopathological change and heat shock protein 70
719 expression in different tissues of Japanese flounder *Paralichthys olivaceus* in response to
720 elevated temperature. *Chin J Oceanol Limn* 33:11-19.
- 721 Zhihao W, Feng Y, Hongjun L, Mengxia L, Jun L, Peijun Z (2012) Effect of waterborne Fe (II) on
722 juvenile turbot *Scophthalmus maximus*: analysis of respiratory rate, hematology and gill
723 histology. *Chin J Oceanol Limn* 30:193-9.



724

725 Fig. 1. Example of a region used to score greenlip abalone (*Haliotis laevis*) gills. This region has
726 relatively normal histopathology and lacks gross lesions, with alignment including the primary
727 rachis (star), the convoluted area of thin epithelium (arrow) and terminating in v-shaped skeletal
728 rods (arrowhead). Bar = 250μm

729 Table 1. Semi-quantitative scoring protocol: Reaction pattern, lesion and assigned importance factor
 730 (ω) for histopathological assessment of greenlip abalone (*Haliotis laevis*) gills.

Reaction Pattern	Lesion	Importance Factor (w)*
Epithelial	Epithelial hypertrophy	1
	Focal epithelial hyperplasia	1
	Goblet cell hyperplasia	1
	Lamellar fusion	2
	Epithelial atrophy	2
	Epithelial lifting at v-shaped skeletal rods	2
	Epithelial necrosis	3
Circulatory	Hemolymph channel enlargement	1
	Vascular congestion	2
	Vascular occlusion	2
	Hemorrhage and rupture of hemolymph channel	3
Inflammation	Hemocyte infiltration	1

731 *Importance factors were assigned based on lesion impact on organ function and reversibility: 1 =
 732 minor pathological importance and can be reversed with improvements to water quality, 2 =
 733 moderate pathological importance and in most cases, can be reversed if water quality is improved, 3
 734 = significant pathological importance, the lesion is irreversible and will lead to either partial or total
 735 loss of organ function (Bernet et al. 1999).

736 Table 2. Reaction pattern, lesions, and the description used for histopathological assessment of
 737 greenlip abalone (*Haliotis laevis*) gills.

Reaction Pattern	Lesion	Description
Epithelial	Epithelial hypertrophy	Increase in size and/or intracellular contents of epithelial cells.
	Focal epithelial Hyperplasia	Increase in the number of epithelial cells at a particular focus point without a change in cell volume or intracellular components.
	Goblet cell hyperplasia	Sporadic increase in the number of clear goblet cells without a change in cell volume or intracellular components.
	Lamellar fusion	Integration of adjacent gill leaflets.
	Epithelial atrophy	Reduction in the size and/or intracellular contents of epithelial cells.
	Epithelial lifting at v- shaped skeletal rods	Visible negative space between epithelial cells and the hemolymph channel of a v-shaped skeletal rod.
	Epithelial necrosis	Visual deterioration of epithelial cells often accompanied by hemocyte infiltration.
Circulatory	Hemolymph channel enlargement	Increase in the width of hemolymph channel.
	Hemorrhage and rupture of hemolymph channel	Obvious rupture of vessels walls, accompanied by the release of excessive hemolymph fluid and hemocytes into the interlamellar space.
	Vascular occlusion	Clotting and organisation of hemocytes within a ballooned hemolymph channel.
	Vascular congestion	Visual clogging and interruption of hemolymph flow often accompanied by hemolymph channel enlargement.
Inflammation	Hemocyte infiltration	Visible migration of hemocytes to lesion and/or significant increase in the number of hemocytes within hemolymph channel.

738

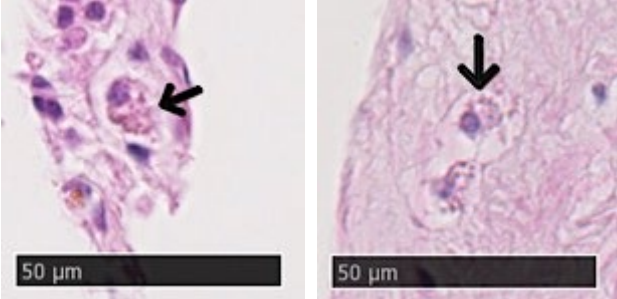
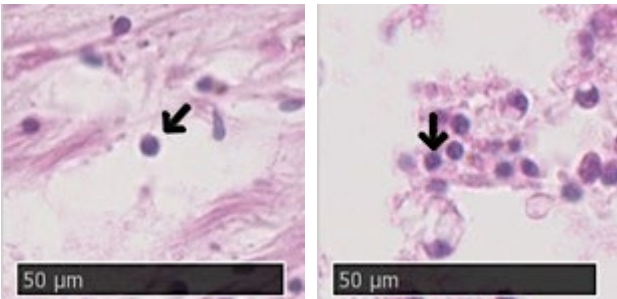
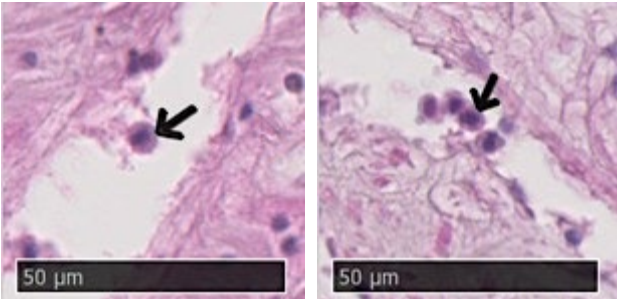
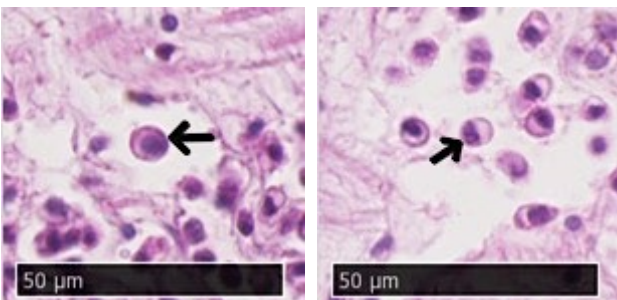
739 Table 3. Lesion score for each prevalence range and its relevant description for histopathological
740 assessment of greenlip abalone (*Haliotis laevis*) gills.
741

Score (a)	Leaflet prevalence range (%)	Description
0	0	No lesions
1	1-19	Minor lesions
2	20-39	
3	40-59	Moderate lesions
4	60-79	
5	80-100	Extensive lesions

742

743 Table 4. Cell types, light microscopy images and descriptions from the hemolymph of greenlip
 744 abalone, *Haliotis laevis*. Arrows point to described features, scale = 50µm.

745

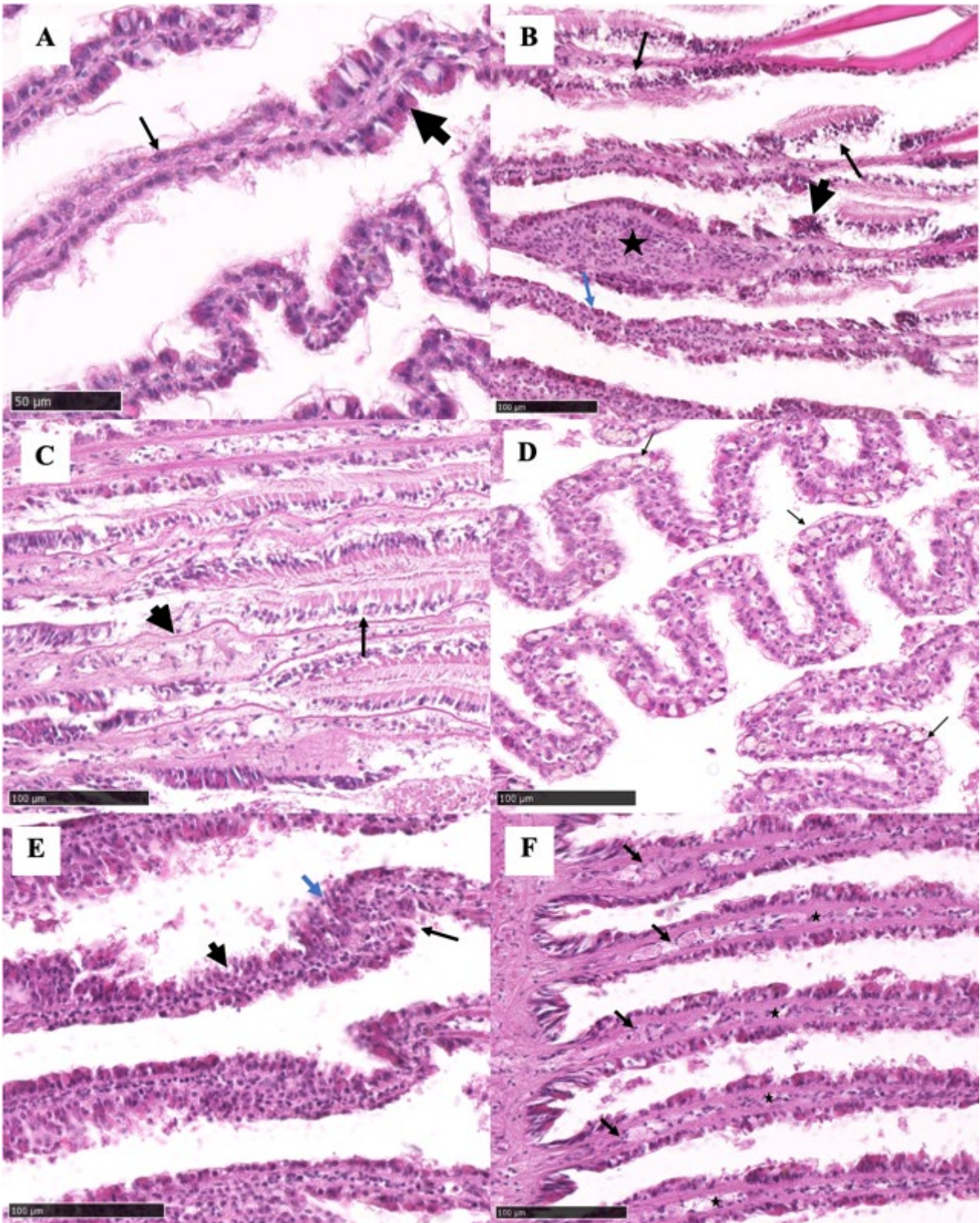
Hemocyte type	Image	Description
Fixed granulocyte		<p>Low nucleus-to-cytoplasm ratio. Large diameter (10-15µm) Granular cytoplasm. Irregular cell shape. Can project pseudopodia.</p>
Small hyalinocyte (blast-like cells)		<p>High nucleus-cytoplasm ratio. Small diameter (2-4µm). Agranular cytoplasm. Round cell shape.</p>
Medium hyalinocyte		<p>Low nucleus-cytoplasm ratio. Moderate diameter (4-6µm). Agranular cytoplasm. Round cell shape.</p>
Large hyalinocyte cell population		<p>Enlarged diameter (5-9µm) and nuclei (3-6µm). High nucleus-cytoplasm ratio. Round cell shape. Some containing mitotic figures.</p>

746 Table 5. Alteration indices (AI) and lesion prevalence (LP) for gills of greenlip abalone (*Haliotis*
 747 *laevigata*) held at either a control (22°C) or elevated temperature (25°C) for 47 days. AI and LP
 748 expressed as mean ± standard deviation.

Reaction Pattern	Lesion	AI		LP (%)	
		22°C	25°C	22°C	25°C
Epithelial	Epithelial hypertrophy	5.80 ± 0.45	4.80 ± 0.84	97.33 ± 5.96	80.00 ± 18.86
	Focal epithelial hyperplasia	4.80 ± 1.64	5.60 ± 0.55	82.67 ± 28.13	94.67 ± 7.30
	Goblet cell hyperplasia	1.20 ± 1.30	1.40 ± 2.07	16.00 ± 19.20	22.67 ± 39.89
	Lamellar fusion	0.00 ± 0.00	0.80 ± 1.30	0.00 ± 0.00	12.00 ± 20.22
	Epithelial atrophy	3.80 ± 1.79	4.20 ± 1.48	60.00 ± 36.82	68.00 ± 29.59
	Epithelial lifting at v-shaped skeletal rods	2.20 ± 1.64 ^A	5.40 ± 0.89 ^B	34.67 ± 28.83 ^a	93.33 ± 11.55 ^b
	Epithelial necrosis	1.40 ± 1.14	2.80 ± 2.59	22.66 ± 20.87	42.67 ± 44.37
Circulatory	Hemolymph channel enlargement	0.80 ± 0.84 ^A	4.60 ± 2.19 ^B	8.00 ± 8.69 ^a	74.67 ± 40.66 ^b
	Hemorrhage and rupture of hemolymph channel	0.40 ± 0.55	1.80 ± 1.30	4.00 ± 5.96	24.00 ± 19.22
	Vascular occlusion	0.40 ± 0.55	1.20 ± 0.84	2.67 ± 3.65	10.67 ± 8.94
	Vascular congestion	0.00 ± 0.00	0.80 ± 1.30	0.00 ± 0.00	9.33 ± 17.38
Inflammation	Hemocyte infiltration	0.60 ± 0.55	4.20 ± 2.68	5.33 ± 5.58	70.67 ± 44.37
		31.40 ± 9.80 ^A		58.80 ± 20.78 ^B	

749 Within rows, different letters in the superscript indicate a statistically significant difference between
 750 temperatures ($p < 0.05$).

751
 752
 753



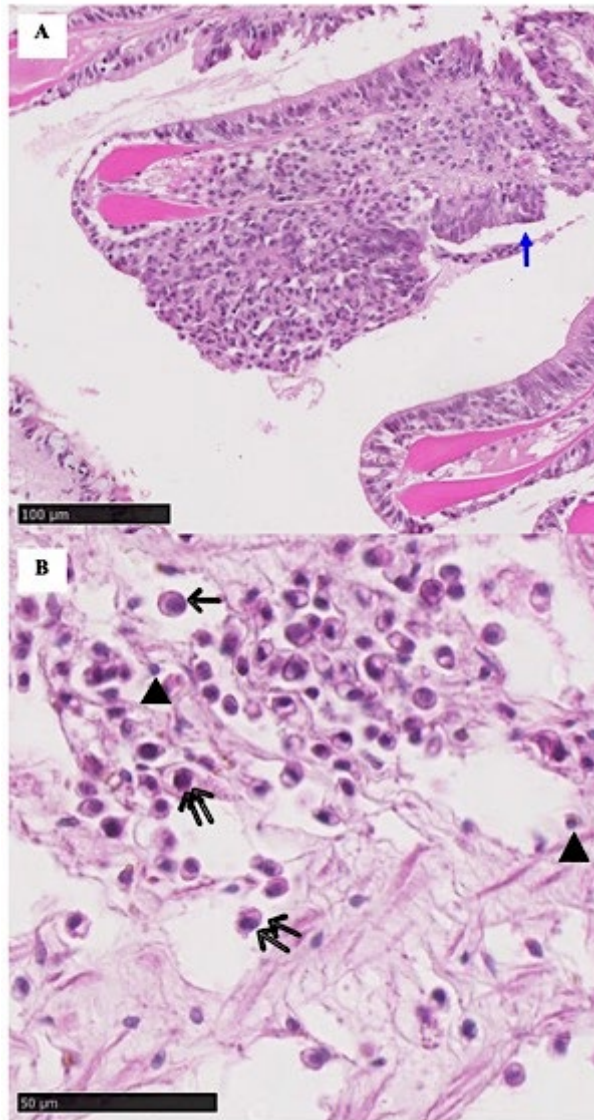
754

755 Fig. 2. Left gill of greenlip abalone (*Haliotis laevis*) displaying multiple lesions. (A) Normal
 756 focus of elongated epithelium proximal to supporting cartilage, with goblet cells containing visible
 757 mucus (black arrowhead), plus other paler cells with unstained mucus, plus mild epithelial swelling
 758 without lifting from the basement membrane in a section of thin convoluted epithelium (black

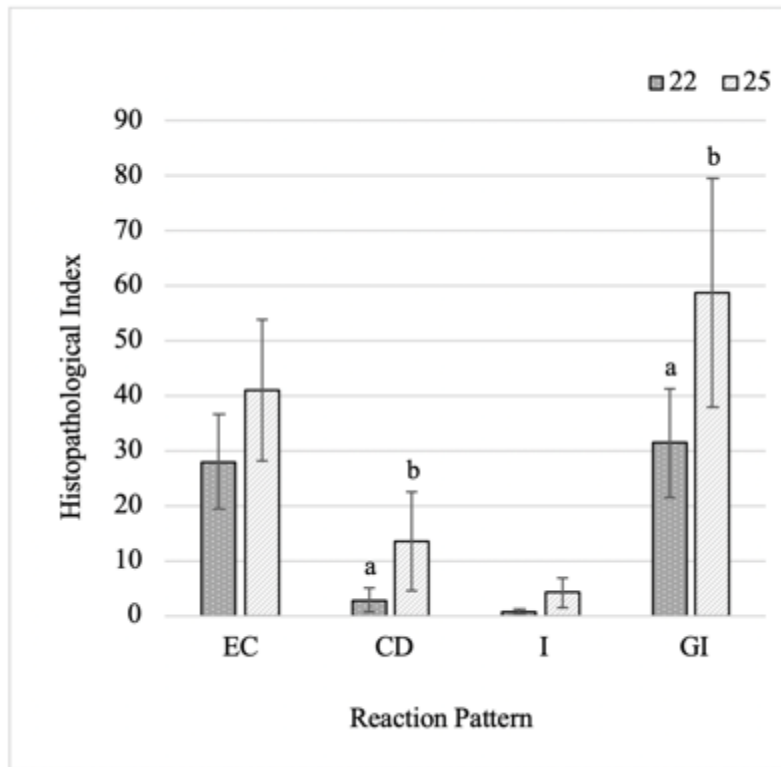
759 arrow). Bar = 50 μ m. (B) vascular occlusion accompanied by hemocyte infiltration (black star),
760 focal disruption and possible hyperplasia of epithelial cells (black arrowhead), epithelial lifting
761 from the basement membrane (black arrow) and disruption of adjacent thin epithelium (blue arrow).
762 Bar = 100 μ m. (C) epithelial lifting (black arrow) with adjacent epithelial loss is severe (epithelial
763 necrosis, black arrow). Remnant epithelial tags suggest this has led to fusion of adjacent gill
764 epithelium. Bar = 100 μ m. (D) goblet cell hyperplasia throughout the length of the thin convoluted
765 epithelium (black arrow), most with pale or unstained mucus. Bar = 100 μ m. (E) Epithelial
766 hypertrophy and fragmentation (mild focal necrosis), (black arrowhead). and epithelial folding
767 (black arrow), opposite a deep fissure in a region of epithelial hyperplasia (blue arrow). Bar =
768 100 μ m. (F) Vascular congestion (black arrow) accompanied by hemolymph channel enlargement
769 (black star). Bar = 100 μ m.

770

771
772
773



774
 775 Fig. 3. (A) Infiltration of hemocytes extending from the v-shaped skeletal rod to a large area of
 776 surface epithelial loss in the gill of greenlip abalone (*Haliotis laevis*). Note the extended margin
 777 suggesting continued cell loss from this area (blue arrow). Bar = 100μm. (B) Enlargement showing
 778 normal (arrowhead) and considerably larger hemocytes (arrow) some of which are illustrating
 779 obvious mitotic figures (double arrow), in the left gill of *H. laevis*. Bar = 50μm.



780
781

782 Fig. 4. Reaction and gill indices (mean \pm SD) for greenlip abalone (*Haliotis laevis*) held at either
783 22°C or 25°C. Indices represented are epithelial (EC), circulatory (CD), inflammatory reaction
784 patterns (I) and overall gill index (GI). Letters indicate significance ($p < 0.05$).